

## REPORT

## Loss of Association of REEP2 with Membranes Leads to Hereditary Spastic Paraplegia

Typhaine Esteves,<sup>1,2,3,4</sup> Alexandra Durr,<sup>1,2,3,5</sup> Emeline Mundwiller,<sup>6</sup> José L. Loureiro,<sup>7</sup> Maxime Boutry,<sup>1,2,3</sup> Michael A. Gonzalez,<sup>8</sup> Julie Gauthier,<sup>9,12</sup> Khalid H. El-Hachimi,<sup>1,2,3,4</sup> Christel Depienne,<sup>1,2,3,5</sup> Marie-Paule Muriel,<sup>1,2,3</sup> Rafael F. Acosta Lebrigio,<sup>8</sup> Marion Gaussen,<sup>1,2,3,4</sup> Anne Noreau,<sup>9</sup> Fiorella Speziani,<sup>8</sup> Alexandre Dionne-Laporte,<sup>9</sup> Jean-François Deleuze,<sup>10</sup> Patrick Dion,<sup>9</sup> Paula Coutinho,<sup>7</sup> Guy A. Rouleau,<sup>9</sup> Stephan Zuchner,<sup>8</sup> Alexis Brice,<sup>1,2,3,5,6</sup> Giovanni Stevanin,<sup>1,2,3,4,6,11,\*</sup> and Frédéric Darios<sup>1,2,3,11,\*</sup>

Hereditary spastic paraplegias (HSPs) are clinically and genetically heterogeneous neurological conditions. Their main pathogenic mechanisms are thought to involve alterations in endomembrane trafficking, mitochondrial function, and lipid metabolism. With a combination of whole-genome mapping and exome sequencing, we identified three mutations in *REEP2* in two families with HSP: a missense variant (c.107T>A [p.Val36Glu]) that segregated in the heterozygous state in a family with autosomal-dominant inheritance and a missense change (c.215T>A [p.Phe72Tyr]) that segregated in *trans* with a splice site mutation (c.105+3G>T) in a family with autosomal-recessive transmission. REEP2 belongs to a family of proteins that shape the endoplasmic reticulum, an organelle that was altered in fibroblasts from an affected subject. In vitro, the p.Val36Glu variant in the autosomal-dominant family had a dominant-negative effect; it inhibited the normal binding of wild-type REEP2 to membranes. The missense substitution p.Phe72Tyr, in the recessive family, decreased the affinity of the mutant protein for membranes that, together with the splice site mutation, is expected to cause complete loss of REEP2 function. Our findings illustrate how dominant and recessive inheritance can be explained by the effects and nature of mutations in the same gene. They have also important implications for genetic diagnosis and counseling in clinical practice because of the association of various modes of inheritance to this new clinico-genetic entity.

Hereditary spastic paraplegias (HSPs) are clinically and genetically heterogeneous inherited neurological disorders mainly characterized by progressive spasticity and, often, loss of vibration sense in the lower limbs.<sup>1,2</sup> These symptoms can be associated in complicated forms of HSP with various other neurological and extraneurological signs.<sup>2,3</sup> The estimated prevalence varies from 1.27 to 9.6/100,000.<sup>4,5</sup> The main pathological characteristic of HSP is the axonal degeneration in the long descending and ascending tracts of the spinal cord, particularly the pyramidal tracts and the dorsal columns, and especially their terminal portions. The clinical heterogeneity of HSP is related to a notable genetic heterogeneity; indeed, more than 50 genetic loci have been identified and mutations have been found in more than 30 genes.<sup>6–8</sup> However, these genes explain only 50% of the cases of HSP, indicating that other genes remain to be discovered. The functions of the proteins encoded by the known genes have suggested that the pathophysiological mechanisms underlying expression of the disease may converge on a small number of cellular functions, including morphogenesis of the endo-

plasmic reticulum, endosomal sorting, mitochondrial function, myelination, or lipid metabolism.<sup>3,6–9</sup>

The endoplasmic reticulum (ER) is a continuous network of membranous sheets and tubules. Its organization is controlled mainly by two families of proteins that have been associated with the pathophysiology of HSPs: the reticulon and REEP/DP1/Yop1p families. The gene encoding reticulon 2 (*RNT2* [MIM 603183]) is mutated in the SPG12 (MIM 604805) subtype of HSP,<sup>10</sup> and mutations in *REEP1* (receptor expression-enhancing protein 1 [MIM 609139]) cause SPG31 (MIM 610250).<sup>11</sup> The proteins of both families have two hydrophobic domains that are thought to form hairpin loops generating curvature of the ER membrane when inserted into the phospholipid bilayer.<sup>12–14</sup> These proteins are thus crucial for the production and stabilization of the highly curved ER tubules and the edges of ER sheets.<sup>13</sup> Accordingly, loss of *Reep1* in a mouse model affected the organization of the ER.<sup>14</sup> Reticulon 2 and REEP1 also interact with two other proteins, atlastin and spastin, implicated in the pathophysiology of SPG3 (MIM 182600) and SPG4 (MIM 182601), respectively.<sup>10,15</sup>

<sup>1</sup>Université Pierre and Marie Curie – Paris VI, Unité Mixte de Recherche S975, Centre de Recherche de l'Institut du Cerveau et de la Moelle épinière, Groupe Hospitalier Pitié-Salpêtrière, 75013 Paris, France; <sup>2</sup>Institut National de la Santé et de la Recherche Médicale, Unité 975, 75013 Paris, France; <sup>3</sup>Centre National de la Recherche Scientifique, Unité Mixte de Recherche 7225, 75013 Paris, France; <sup>4</sup>Laboratoire de Neurogénétique, Ecole Pratique des Hautes Etudes, Institut du Cerveau et de la Moelle épinière, Groupe Hospitalier Pitié-Salpêtrière, 75013 Paris, France; <sup>5</sup>APHP, Centre de Génétique Moléculaire et Chromosomique, Groupe Hospitalier Pitié-Salpêtrière, 75013 Paris, France; <sup>6</sup>Institut du Cerveau et de la Moelle épinière, Groupe Hospitalier Pitié-Salpêtrière, 75013 Paris, France; <sup>7</sup>UnIGENE and Centro de Genética Preditiva e Preventiva, Institute for Molecular and Cellular Biology, 4050 Porto, Portugal; <sup>8</sup>Department of Human Genetics and Hussman Institute for Human Genomics, Miller School of Medicine, University of Miami, Miami, FL 33136, USA; <sup>9</sup>Montreal Neurological Institute and Hospital, Department of Neurology and Neurosurgery, McGill University, Montreal, QC H3A 2B4, Canada; <sup>10</sup>Centre National de Genotypage, 91057 Evry, France

<sup>11</sup>These authors contributed equally to this work

<sup>12</sup>Present address: Molecular Diagnostic Laboratory and Division of Medical Genetics, CHU Sainte-Justine, Montreal, QC H3T 1C5, Canada

\*Correspondence: [giovanni.stevanin@upmc.fr](mailto:giovanni.stevanin@upmc.fr) (G.S.), [frederic.darios@upmc.fr](mailto:frederic.darios@upmc.fr) (F.D.)

<http://dx.doi.org/10.1016/j.ajhg.2013.12.005>. ©2014 by The American Society of Human Genetics. All rights reserved.

Here we report the identification of mutations in the gene encoding another member of the REEP/DP1/Yop1p family, receptor expression-enhancing protein 2 (*REEP2*), in two families, one with autosomal-dominant HSP and the other with autosomal-recessive inheritance of the disease. In addition, we present evidence that loss of the ability of *REEP2* to bind to membranes underlies the disease.

Two families with HSP were selected according to the Harding's criteria,<sup>1</sup> after exclusion of alternative causes, and were sampled for DNA extraction. All family members were informed and signed consent according to the Paris-Necker Ethics Committee approval (RBM INSERM n°01-29).

Family FSP200 is a French family with ten living affected individuals, four at-risk subjects, and two healthy spouses (Figure 1A and Table S1 available online). All affected subjects had a homogeneous, pure HSP phenotype (spastic gait and mild stiffness at rest) since childhood (mean age at onset of  $3.7 \pm 1.9$  years). At the time of examination ( $32.9 \pm 20.9$  years), after a mean disease duration of  $28.0 \pm 9.1$  years, sphincter disturbance was noted in five subjects, pes cavus in three, a slight postural tremor in two, and decreased vibration sense at ankles in two. The index subject (FSP200-IV.4) also complained of diffuse pain and problems with memory and concentration at age 59. The disease progressed slowly as evaluated with the spastic paraplegia rating scale<sup>16</sup> in the index subject (scores of 19/52 and 21/52 at ages 54 and 59, respectively). The three subjects with the longest disease durations (43, 55, and 61 years) were still able to walk without help or with unilateral assistance. No cerebellar syndrome, mental impairment, or ocular abnormalities were observed. Mutations in *SPAST* (SPG4) and *HSPD1* (SPG13 [MIM 605280]) were excluded by direct Sanger sequencing, and genome-wide linkage mapping with SNP markers covering all chromosomes (Illumina LINKAGE\_12 microarrays) was undertaken to localize the mutation responsible for the disease, as previously described.<sup>17</sup> Linkage analysis, assuming a dominant inheritance model with incomplete penetrance set at 80%, identified 42 chromosomal regions covering a total of 235 Mb putatively segregating with the disease: eight regions with positive multipoint LOD scores ranging from +0.5 to +2.1 on chromosomes 4, 5, 12, 19, and X and 34 uninformative regions with LOD scores ranging from -1.9 to +0.1. Only one region overlapped with a known SPG candidate region, *SPG36* (MIM 613096).<sup>18</sup> We used this information to filter the exome-sequencing data from three affected individuals (FSP200-IV.1, FSP200-V.7, and FSP200-V.8) as described elsewhere.<sup>19</sup> Variants in the heterozygous state were selected according to their quality (GATK quality score > 30),<sup>20</sup> functional class (nonsynonymous and/or affecting splicing), presence in chromosomal regions with putative or nonexcluded linkage, and frequency  $\leq 0.1\%$  in publically available genomic databases (dbSNP135, NHLBI). These criteria reduced the list to two missense variants (Table S2): (1) c.483G>T

(p.Leu161Phe) in *SERPINA1* (RefSeq accession number NM\_001002236.2) that was considered tolerated/benign by SIFT, Mutation Taster, and PolyPhen-2 algorithms and altered an amino acid not conserved in primates; and (2) c.107T>A (p.Val36Glu) in *REEP2* (RefSeq NM\_016606.3, Figures 1B and 1C), which segregated with the disease in the family (Figure 1A), was predicted to be deleterious by the same algorithms as above and affected an amino acid conserved up to *D. melanogaster* and *C. elegans* and in the paralogous human proteins REEP1, REEP3, and REEP4 (Figure 1D). This mutation was also absent from an in-house exome data set of 2,615 individuals with various unrelated neurological disorders. Of note, one asymptomatic subject with the mutation (FSP200-V.2, Figure 1A) was 23 years old at last examination and was considered to be possibly affected because of brisk reflexes in the lower limbs, pes cavus, and no plantar response, in the absence of spastic gait.

Family FSP940 is a Portuguese family in which four affected children were born of unaffected, nonconsanguineous parents (Figure 1A). One of these children died before the genetic studies but was clinically assessed. The four affected subjects had a pure HSP phenotype (Table S1) since the age of 2, which worsened with time, but not at the same rate; the affected individuals needed two canes to walk after disease durations varying from 6 to 23 years. To identify the mutations responsible for HSP in this kindred, we used the same strategy as for family FSP200, a combination of whole-genome linkage mapping and exome sequencing. The whole-genome linkage analysis, assuming a fully penetrant recessive mode of inheritance, detected 433 Mb of the genome that segregated in all affected subjects at an identical state: in five chromosomal regions, multipoint LOD scores ranged from +0.5 to +0.9; in six regions, the multipoint LOD scores reached the maximal expected value of +1.2 in the pedigree (chromosomes 1, 2, 5, 9, 10, 15); 75 regions were uninformative with LOD scores between -1.9 and +0.2. Some of these regions partially overlapped with known autosomal-recessive or X-linked SPG loci, namely *SPG16* (MIM 300266), *SPG27* (MIM 609041), and *SPG45* (MIM 613162).<sup>21-23</sup> Exome sequencing in subjects FSP940-III.2 and FSP940-III.3 was then performed as in family FSP200. The same analytic criteria were applied except that we focused on homozygous or compound heterozygous variants (frequency < 1% in public databases) in conformity with the most likely mode of inheritance in this kindred (Table S2). No homozygous variants were found in the putatively linked or uninformative regions, and only one gene, *REEP2*, had two heterozygous mutations in both affected cases: (1) a c.105+3G>T change that was predicted (Splice Site Finder algorithm) to alter the 5' consensus splicing sequence of intron 2; and (2) a c.215T>A missense change (p.Phe72Tyr) (Figure 1C), predicted to be deleterious by PolyPhen-2 and Mutation Taster (and tolerated by SIFT) and affecting an amino acid conserved during evolution of *REEP2* (up to the

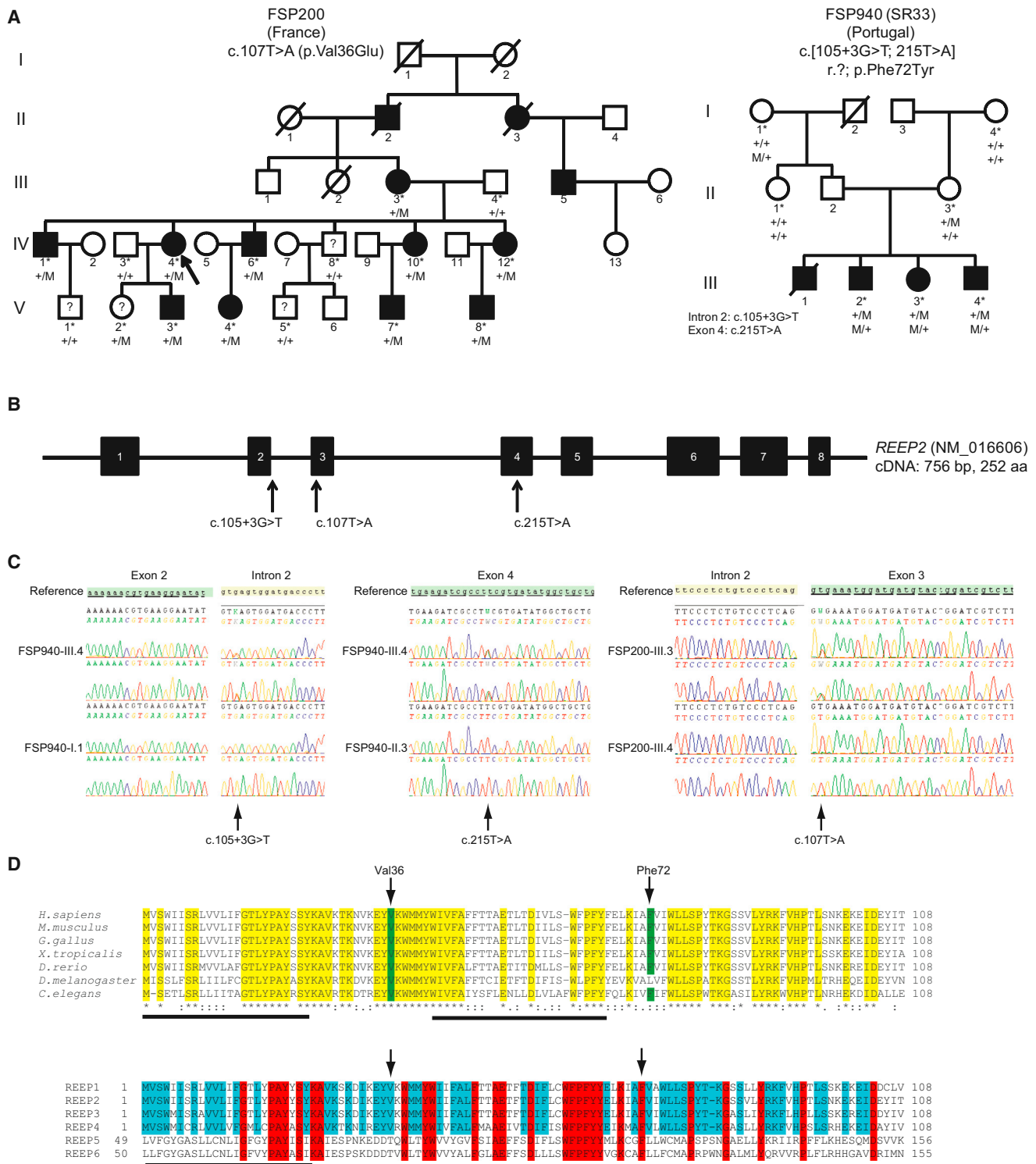


**Figure 1. Pedigrees and Segregation of the REEP2 Mutations**

(A) Pedigrees of two families with hereditary spastic paraplegia. Segregation of the mutations is indicated (plus sign indicates wild-type, M indicates mutation). Affected individuals are designated by black squares (men) or circles (women). Sampled individuals are designated by an asterisk (\*). Subjects with unknown status are designated with a question mark. The arrow indicates the index subject.

(B) Schematic representation of the gene showing the sites of the mutations.

(C) Electrophoregrams showing the mutations.

(D) Conservation of amino acids in the N-terminal domain of REEP2 according to the phylogenetic evolutionary tree (top) and in comparison with other members of the REEP family in *H. sapiens*. The positions of the missense mutations are shown by arrows. Conserved amino acids are in yellow (among species), red (among all REEP proteins), or blue (among members of the REEP1–REEP4 subfamily). Horizontal bars represent the hydrophobic segments of the proteins.

zebrafish) and in all members of the REEP family (Figure 1D). Both mutations were absent from the exome of 76 healthy controls and 2,615 individuals affected by various neurological disorders. The effect of the splice site mutation could not be verified in mRNA from affected subjects.

The three mutations identified in *REEP2* are likely to be pathogenic for the following reasons. (1) They were absent from a large series of controls and local or public exomes, including 500 index subjects with hereditary spastic paraplegia or peripheral neuropathy. (2) They segregated with the disease in the heterozygous (c.107T>A [p.Val36Glu]) or compound heterozygous (c.[105+3G>T; 215T>A], r.?: p.Phe72Tyr) state according to the type of inheritance suspected in the pedigrees. (3) They were the only variants remaining after filtering of the exome data obtained with high base coverage (Table S2). (4) The mutations led (theoretically) to missplicing (c.105+3G>T) or affected amino acids that are highly conserved during evolution, even among paralogous members of the REEP family, suggesting that they impair the functions of the protein. (5) Another member of the REEP family, *REEP1*, is mutated in SPG31 HSP<sup>11</sup> and the two *REEP2* missense variants are located in the highly conserved hydrophobic N-terminal domain of the protein, as are all of the missense mutations reported so far in *REEP1*.<sup>11,24–27</sup>

*REEP2* is highly expressed in brain and testis.<sup>28</sup> Its product, REEP2, together with REEP1, belongs to the DP1/Yop1p family of ER-shaping proteins. The proteins of this family contain two highly conserved hydrophobic domains at their N terminus, which have been suggested to form hairpins that insert into membranes and promote homo- or hetero-oligomerization.<sup>15,29</sup> Insertion of hairpins into membranes can modulate their curvature;<sup>12–14</sup> loss of *Reep1* in a mouse model indeed affected the organization of the ER.<sup>14</sup> Furthermore, several proteins of the REEP/DP1/Yop1p family have been shown to interact with microtubules. This interaction is mediated by the carboxyl terminus of the protein in REEP1<sup>15</sup> or by basic residues between the two hydrophobic domains in REEP3 and REEP4.<sup>30</sup> Because the p.Val36Glu and p.Phe72Tyr variants associated with HSP in families FSP200 and FSP940 affect conserved residues in the N-terminal domain of REEP2, we hypothesized that these variants may affect the ER-shaping properties of REEP2.

We first analyzed the consequences of the p.Val36Glu substitution on the subcellular localization of the protein. When we overexpressed V5-tagged REEP2 in COS7 cells, both the wild-type and the p.Val36Glu variants were distributed in a dot-like pattern along both the ER and the microtubules (Figure S1). Of note, unlike previous observations,<sup>15</sup> REEP2 rarely induced the formation of microtubule bundles (less than 2% of cells) and this occurred only in cells expressing the highest levels of REEP2. The subcellular localization of REEP2 was therefore consistent with a possible role for the protein in ER shaping.

We therefore analyzed ER morphology in primary fibroblasts from the affected subject FSP200-IV.4 that expressed the p.Val36Glu variant. The levels of REEP2 in FSP200-IV.4's fibroblasts were similar to those in age-matched control fibroblasts (Figure 2A). We then transfected the fibroblasts with a vector allowing expression of GFP-Sec61 $\beta$ <sup>12</sup> to label the whole ER and immunolabeled them with an antibody against the ER sheet protein CLIMP-63.<sup>13</sup> In control fibroblasts, CLIMP-63 immunoreactivity was concentrated around the nucleus and was almost absent from peripheral ER. In contrast, in FSP200-IV.4's fibroblasts, CLIMP-63 staining was interspersed throughout the GFP-Sec61 $\beta$  labeling (Figure 2B). In FSP200-IV.4's fibroblasts, the percentage of the cellular area occupied by CLIMP-63 staining was significantly increased compared to control fibroblasts, indicating that CLIMP-63 was distributed more widely throughout peripheral ER and that ER sheets were expanded (Figure 2C). To further investigate the consequences of the p.Val36Glu substitution in REEP2, we analyzed the fibroblasts by transmission electron microscopy (Figure 2D) as previously described.<sup>31</sup> In control fibroblasts, most ER structures were 20 to 60 nm thick, as expected.<sup>13</sup> In contrast, ER tubules thinner than 20 nm and swollen ER sheets thicker than 100 nm were more numerous in fibroblasts containing mutant REEP2 (Figure 2E).

Because the level of REEP2 in FSP200-IV.4's fibroblasts was similar to control level (Figure 2A), the observed phenotype could be due either to haploinsufficiency caused by loss of function of the p.Val36Glu variant or to a dominant-negative gain of function. To test these hypotheses, we downregulated the expression of REEP2 in COS7 cells by using shRNA vectors (Figure 3A) and immunostained the cells with antibodies against calreticulin and CLIMP-63 to visualize the organization of the ER. As observed in FSP200-IV.4's fibroblasts, CLIMP-63 staining was widely distributed after downregulation of REEP2 (Figures 3B and 3C). We then tested the effect of the p.Val36Glu variant on ER morphology in COS7 cells by overexpressing wild-type or p.Val36Glu REEP2. The distribution of CLIMP-63 was similar in nontransfected cells and those overexpressing wild-type REEP2 but was more widespread in cells overexpressing p.Val36Glu REEP2 (Figures 3D and 3E). This demonstrated that overexpression of p.Val36Glu REEP2 led to a phenotype similar to that observed in fibroblasts from the affected subject (Figure 2B).

The similarity between the phenotypes induced by downregulation of REEP2 or overexpression of the p.Val36Glu REEP2 variant suggested that p.Val36Glu might inhibit the function of endogenous wild-type REEP2, possibly by interfering with its ability to form oligomers like other proteins of the REEP/DP1/Yop1p family.<sup>15,29</sup> To investigate how the p.Val36Glu variant might affect REEP2, we focused on properties probably mediated by its N-terminal domain: protein-protein interactions, binding to microtubules, and binding to membranes.



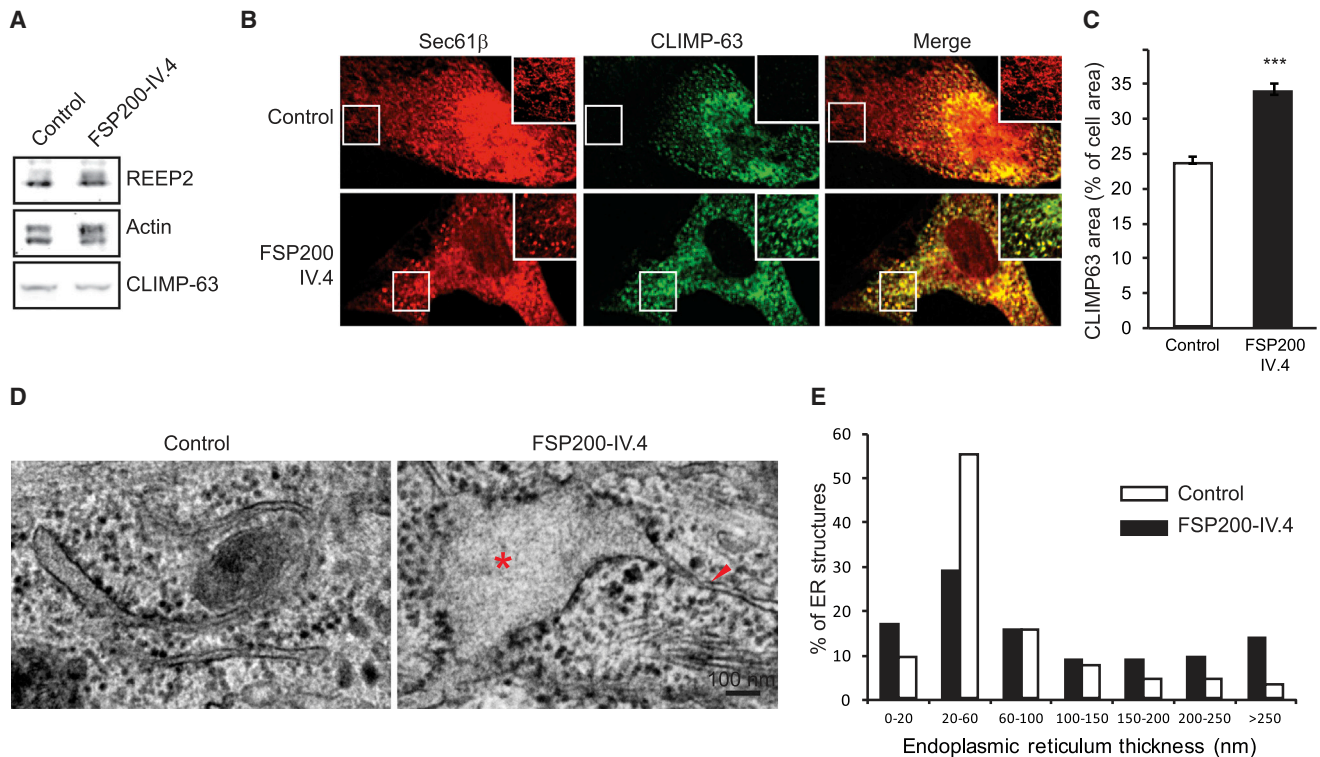


**Figure 2. REEP2 Is Implicated in ER Morphogenesis**

(A) Immunoblot showing the amount of endogenous REEP2, actin, and CLIMP-63 in fibroblasts from a control and family member FSP200-IV.4.

(B) Control and FSP200-IV.4 fibroblasts were transfected with vectors directing expression of GFP-Sec61β (red, false color) and immunostained with antibodies against CLIMP-63 (green).

(C) Quantification of the area occupied by CLIMP-63 staining in cells (control  $n = 50$ , FSP200-IV.4  $n = 57$ ). Data represent mean  $\pm$  SEM. \*\*\* $p < 0.0001$ ,  $t$  test.

(D) Transmission electron micrographs of control and FSP200-IV.4 fibroblasts. Asterisk indicates swollen ER; arrowhead points to a very thin ER sheet.

(E) Quantification of the thickness of ER sheets in fibroblasts. Control  $n = 210$ , FSP200-IV.4  $n = 237$ . \*\*\* $p = 4 \times 10^{-8}$ , chi-square test.

We first investigated whether the p.Val36Glu variant modified an interaction with wild-type REEP2 by cotransfecting COS7 cells with vectors directing expression of V5- and GFP-tagged REEP2. Both proteins coimmunoprecipitated with an anti-V5 antibody, and the p.Val36Glu variant did not prevent the interaction between the mutant and the wild-type protein (Figure S2A). We then cotransfected cells with vectors directing expression of REEP2 in combination with atlastin-1, M1-spastin, or REEP1. Atlastin, M1-spastin, and REEP1 coimmunoprecipitated with REEP2, even in the presence of p.Val36Glu REEP2 variant (Figures S2B–S2D). We also assessed the interaction of REEP2 with microtubules in extracts from COS7 cells overexpressing REEP2, by using an *in vitro* microtubule pull-down assay. Both wild-type and p.Val36Glu REEP2 interacted with microtubules (Figure S3).

Finally, to monitor the interaction of REEP2 with membranes, we performed a subcellular fractionation in COS7 cells expressing V5-tagged REEP2 as previously described.<sup>15</sup> Wild-type and p.Val36Glu REEP2 sedimented in the membrane fraction (Figure 4A). Upon alkaline extraction,<sup>15</sup> both wild-type and mutated REEP2 disso-

ciated from membranes in a manner similar to the membrane-associated protein calreticulin (Figure 4B). This suggests that REEP2, in contrast to REEP1, is not an integral membrane protein. The binding of REEP2 to membrane could thus be mediated either by a labile interaction or by interaction with integral membrane proteins such as REEP1, atlastin, or spastin. To discriminate among these possibilities, we purified recombinant REEP2 from *E. coli* extracts as previously described<sup>32</sup> and used a liposome flotation assay to analyze its ability to bind to membranes in the absence of any other protein.<sup>32</sup> We observed that a portion of wild-type REEP2 bound to membranes, whereas the p.Val36Glu variant did not (Figures 4C–4E). Importantly, when the assay was performed with an equimolar mixture of wild-type and p.Val36Glu REEP2, the interaction with membranes was abolished, suggesting that the presence of p.Val36Glu variant impeded binding of the wild-type protein to membranes.

The data obtained with the p.Val36Glu variant show that REEP2 must interact with integral membrane proteins to sediment in the subcellular membrane fraction. This interaction might concentrate REEP2 in proximity

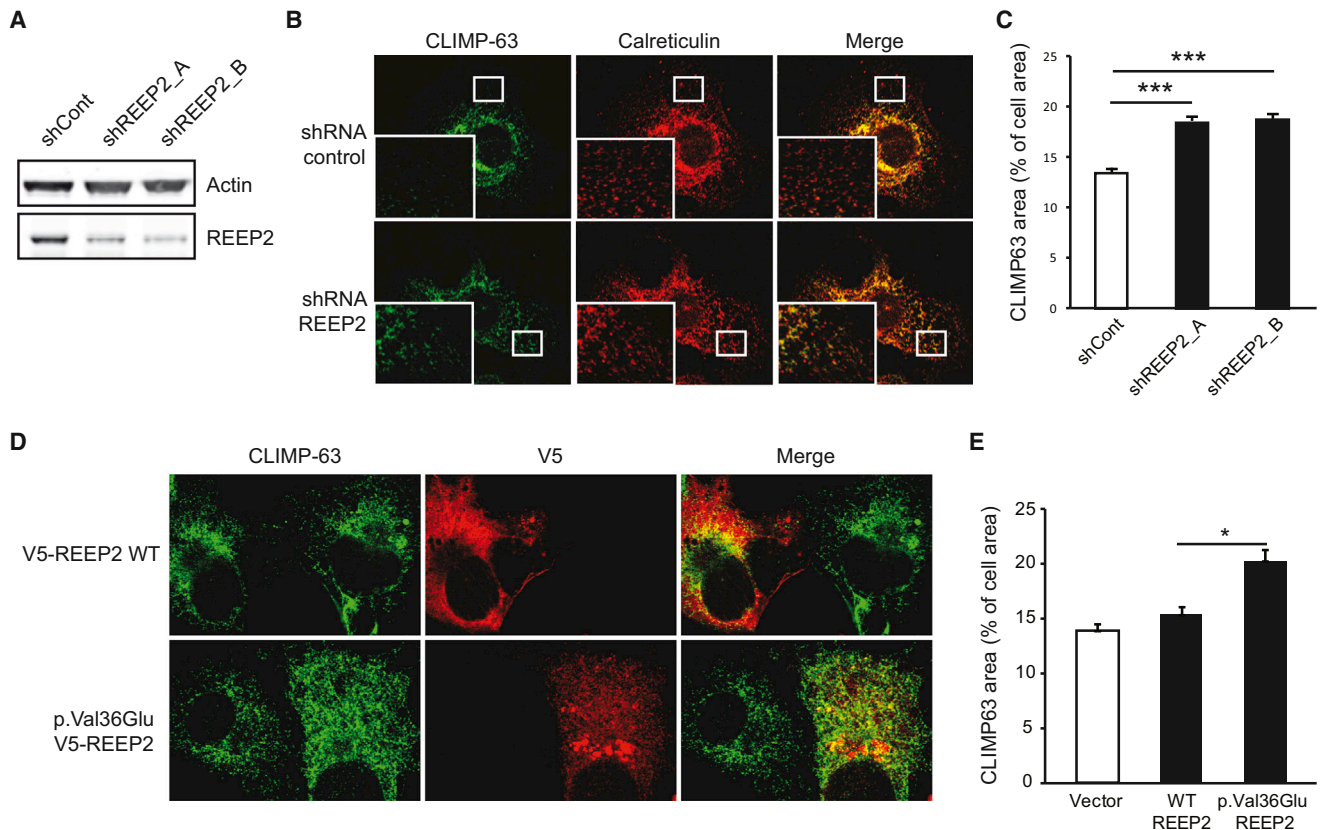


**Figure 3. REEP2 Downregulation Leads to Expansion of ER Sheets**

(A) COS7 cells were transfected with vectors directing the expression of shRNAs obtained from Sigma (shRNA REEP2\_A hairpin sequence: CCCAGCCTATTCTCTCTACAACCTCGAGTTGTAGGAAGAATAGGCTGGGT, shRNA REEP2\_B hairpin sequence: ACTGGCTTCCAAGACACTGAACCTCGAGTTCAGTGTCTTGGAGCCAGTT). Cell lysates were immunoblotted with antibodies against endogenous REEP2 and actin.

(B) COS7 cells in which endogenous REEP2 was downregulated by shRNA were immunostained with antibodies against the endoplasmic reticulum marker calreticulin and CLIMP-63 that labels ER sheets.

(C) Quantification of the area occupied by CLIMP-63 staining in cells.  $n > 50$  cells in three independent experiments. Data represent mean  $\pm$  SEM. \*\*\* $p < 0.001$ , one-way ANOVA.

(D) COS7 cells were transfected with vectors directing the expression of wild-type or V5-tagged p.Val36Glu REEP2. Cells were immunostained with anti-V5 and anti-CLIMP-63 antibodies.

(E) Quantification of the cellular area occupied by CLIMP-63 staining.  $n > 50$  cells per condition. Data represent mean  $\pm$  SEM. \* $p < 0.05$ , one-way ANOVA.

to membranes. However, the ability of REEP2 to interact directly with membranes is more probably due to insertion of its hydrophobic regions into membranes, modulating membrane curvature as shown for REEP1.<sup>14</sup> The simultaneous presence of the p.Val36Glu variant and wild-type REEP2, which recapitulates the situation observed in FSP200 family, abolishes the direct interaction of the latter with membranes, thus preventing REEP2 from regulating membrane curvature in ER tubules or at the edges of ER sheets where the protein is localized. These data are consistent with the ER sheet expansion and ER swelling observed in cells expressing p.Val36Glu REEP2 and confirm that this variant induces loss of function of the wild-type REEP2 through a dominant-negative effect. It could thus underlie the physiopathology of HSP in family FSP200.

We then investigated whether such a loss-of-function mechanism could also occur in family FSP940, with

two heterozygous mutations in REEP2: a splice-site mutation and missense change affecting a conserved residue (p.Phe72Tyr). Because the splice site mutation very probably prevents the expression of a functional protein, we focused on the consequences of the p.Phe72Tyr substitution in REEP2. After overexpression in COS7 cells, V5-tagged p.Phe72Tyr REEP2 was distributed along ER and microtubules (Figure S1) like the wild-type protein. Microtubule pull-down experiments performed with extracts from COS7 cells overexpressing p.Phe72Tyr REEP2 demonstrated that the p.Phe72Tyr variant was able to bind to microtubules like the wild-type protein (Figure S3). Coimmunoprecipitation of REEP1 and V5-tagged REEP2 from COS7 cells overexpressing these proteins showed that p.Phe72Tyr REEP2 coimmunoprecipitated about 25% less REEP1 than did wild-type REEP2 or the p.Val36Glu variant (Figures 4F and 4G). In subcellular fractionation experiments, p.Phe72Tyr REEP2

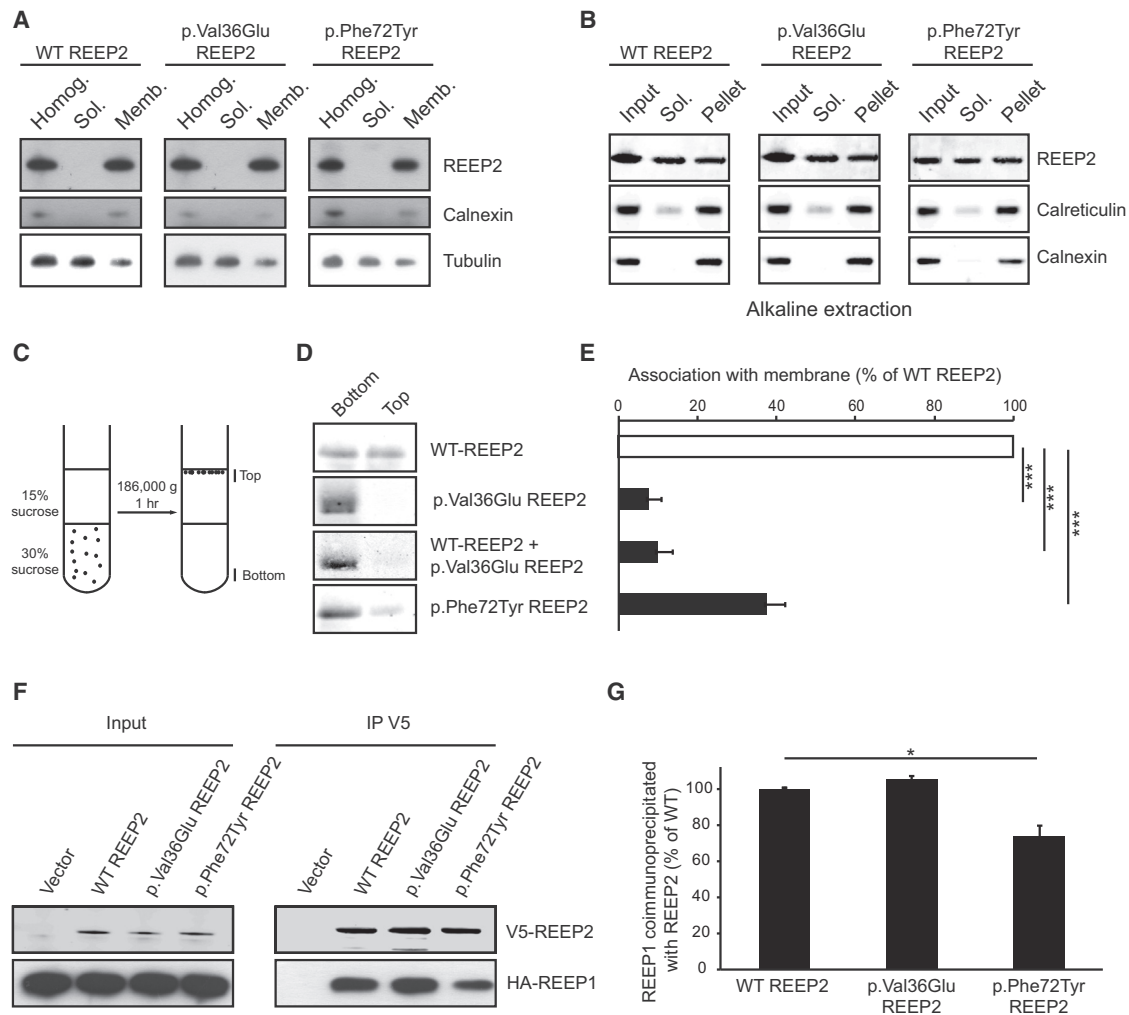


**Figure 4. Interaction of REEP2 with REEP1 and Membranes**

(A) Homogenates (Homog.) from V5-tagged REEP2-expressing COS7 cells were separated into soluble (Sol.) and membrane (Memb.) fractions and then immunoblotted to detect REEP2 (anti-V5 antibody), the membrane marker calnexin, and the cytosolic marker tubulin. (B) Lysed membranes from V5-tagged REEP2-expressing COS7 cells were subjected to alkaline extraction, and the soluble and pellet fractions were analyzed by immunoblot to detect REEP2 (anti-V5 antibody), the soluble protein calreticulin, and the integral membrane protein calnexin.

(C) Schema representing the liposome flotation experiment. Liposomes were prepared by mixing chloroform solutions of brain phosphatidylcholine and phosphatidylserine (Avanti Polar Lipids) in 75:25 ratio. After drying the lipids under nitrogen, they were resuspended in 100 mM NaCl, 10 mM Tris (pH 7.4) and sonicated. Liposomes were incubated with recombinant protein for 30 min at 22°C, and then mixed with equal amount of 50% sucrose in 100 mM NaCl, 10 mM Tris (pH 7.4). The mixture was overlaid with 40  $\mu$ l of 15% sucrose solution. After centrifugation, the liposomes were collected at the top of the upper phase (top) and unbound proteins in the lower phase (bottom).

(D) Liposome flotation assay with wild-type REEP2, p.Val36Glu REEP2, p.Phe72Tyr REEP2, and an equimolar amount of wild-type and p.Val36Glu REEP2 analyzed by immunoblot with an antibody raised against REEP2.

(E) Quantification of the association of recombinant REEP2 with membranes. Data represent mean  $\pm$  SEM (n = 4). \*\*\*p < 0.001, one-way ANOVA.

(F) V5-tagged REEP2 and HA-tagged REEP1 were coexpressed in COS-7 cells and REEP2 immunoprecipitated with an anti-V5 antibody. The eluates were analyzed by immunoblot.

(G) Quantification coimmunoprecipitation of HA-REEP1 with REEP2. The p.Phe72Tyr variant in REEP2 decreased the interaction of REEP2 with REEP1. Data represent mean  $\pm$  SEM (n = 3). \*p < 0.05.

sedimented with membranes (Figure 4A). It should be noted that these experiments were performed in the presence of the wild-type protein expressed by COS7 cells. This could partially mask the pathogenic effect of the mutation in cells of affected members of family FSP940 in which the second mutated allele is probably degraded

at the mRNA level, resulting in downregulation of the protein. We then assessed the ability of the recombinant protein to directly bind to liposome membranes in an in vitro assay. The p.Phe72Tyr variant associated with membranes, but with a much lower affinity than the wild-type protein (Figures 4C–4E), suggesting that the p.Phe72Tyr

substitution induced the loss of this function. Because the mutation encoding this variant is associated in *trans* with a splice site mutation, we hypothesize that it would cause a strongly decreased association of REEP2 with membrane in affected members of family FSP940, which fits well with the autosomal-recessive inheritance observed in this family.

In conclusion, we have identified mutations in *REEP2* in two families with relatively pure, early-onset HSP, one with autosomal-dominant and the other with autosomal-recessive transmission. In family FSP200, we demonstrated that the mutant protein inhibited the direct binding of wild-type REEP2 to membranes, in agreement with a dominant-negative effect of the mutation on this property. In family FSP940, the splice site mutation is expected to decrease expression of the protein by 50%, whereas the second mutation, expressed in *trans*, affects the membrane binding properties of the protein. This would lead to a complete loss of membrane binding by REEP2. The loss of interaction of REEP2 with membranes could thus be a common mechanism in autosomal-dominant and -recessive inherited cases of this HSP subtype. The ability of REEP2 to bind directly to membranes is probably due to the insertion of its hydrophobic domains into the phospholipid bilayer. As shown for other members of this family of proteins,<sup>12–14</sup> this property might regulate the curvature of ER membranes where the protein resides. Loss of this function would lead to a decrease in ER membrane curvature, explaining the expansion of ER sheets and ER swelling observed in fibroblasts from an affected individual. Other proteins of the REEP/DP1/Yop1p family probably partially compensate for the loss of REEP2 function, explaining why we did not detect the massive proliferation of ER sheet observed in *S. cerevisiae* lacking both reticulon and Yop1p.<sup>12</sup> We also cannot exclude that other functions of the REEP2 protein may contribute to the phenotype, as for example, the reduced interaction of p.Phe72Tyr REEP2 with REEP1 shown in our study. REEP2 has also been proposed to modulate the trafficking of proteins from ER to Golgi.<sup>33</sup> It is thus possible that the loss of REEP2 association with membrane and the alteration of ER morphology observed in cells of affected subjects would change this trafficking activity and that this could also contribute to the pathology.

These findings illustrate how the nature of the mutations and their effects determine the mode of transmission of a genetic trait. Various modes of transmission associated to mutations in a single gene have been shown in other diseases,<sup>34</sup> including other forms of spastic paraplegia, e.g., SPG7 (MIM 607259).<sup>35</sup> One can speculate that deciphering the deleterious effects of the mutations in *SPG7* (MIM 602783) would explain why dominant inheritance is associated with isolated optic atrophy whereas recessive inheritance leads to a more complex phenotype including spastic paraplegia, optic atrophy, and various degrees of cerebellar involvement.

## Supplemental Data

Supplemental Data include three figures and two tables and can be found with this article online at <http://www.cell.com/AJHG/>.

## Acknowledgments

We first of all thank the family members that kindly participated in this study. We also thank Imed Feki who performed some clinical examinations, Merle Ruberg for the critical reading of the manuscript, and Isabel Alonso, Sara Morais, Eva Brandao, and Céline Lustremant for their help. We are also grateful to Craig Blackstone (NINDS, Bethesda, MD) and Gia K. Voeltz (University of Colorado, Boulder, CO) for the REEP1 and GFP-Sec61 $\beta$  expression vectors, respectively. Some aspects of this work were performed thanks to the contribution of the DNA and Cell Bank (coordinators Sylvie Forlani and A.D.) of the Centre de Recherche de l'Institut du Cerveau et de la Moelle épinière (ICM), the genomic P3S facility (coordinators Wassilla Carpentier and Florent Soubrier), the ICM genotyping/sequencing facility (coordinators Yannick Marie and G.S.), and the Plateforme d'Imagerie Cellulaire de la Pitié-Salpêtrière. This study was funded by the program "Investissements d'avenir" ANR-10-IAIHU-06 (to the Institut du Cerveau et de la Moelle épinière), the Verum Foundation (to A.B.), the French Agency for Research (ANR) (to G.S. and A.D.), the Association Française contre les Myopathies (to G.S.), The Fondation Roger de Spoelberch (R12123DD to A.B.), the Canadian Institutes of Health Research (to G.A.R.), the National Institutes of Health (R01NS072248 and R01NS072248S1/S2 to S.Z. and M.G.), and the European Union with the ANR (E12009DD to A.B., Seventh Framework Program - FP7, Omics call) and with the European Research Council (ERC, Starting grant No 311149 to F.D.).

Received: November 11, 2013

Accepted: December 9, 2013

Published: January 2, 2014

## Web Resources

The URLs for data presented herein are as follows:

1000 Genomes, <http://browser.1000genomes.org>  
 Alamut, <http://www.interactive-biosoftware.com/>  
 Berkeley Drosophila Genome Project NNSplice 0.9, [http://www.fruitfly.org/seq\\_tools/splice.html](http://www.fruitfly.org/seq_tools/splice.html)  
 dbSNP, <http://www.ncbi.nlm.nih.gov/projects/SNP/>  
 GEM.app, <https://genomics.med.miami.edu>  
 ImageJ, <http://rsbweb.nih.gov/ij/>  
 Mutalyzer, <https://mutalyzer.nl/index>  
 MutationTaster, <http://www.mutationtaster.org/>  
 NHLBI Exome Sequencing Project (ESP) Exome Variant Server, <http://evs.gs.washington.edu/EVS/>  
 Online Mendelian Inheritance in Man (OMIM), <http://www.omim.org/>  
 PolyPhen-2, <http://www.genetics.bwh.harvard.edu/pph2/>  
 RefSeq, <http://www.ncbi.nlm.nih.gov/RefSeq>  
 SIFT, <http://sift.bii.a-star.edu.sg/>

## References

- Harding, A.E. (1983). Classification of the hereditary ataxias and paraplegias. *Lancet* *1*, 1151–1155.



2. Tallaksen, C.M., Dürr, A., and Brice, A. (2001). Recent advances in hereditary spastic paraplegia. *Curr. Opin. Neurol.* 14, 457–463.
3. Stevanin, G., Ruberg, M., and Brice, A. (2008). Recent advances in the genetics of spastic paraplegias. *Curr. Neurol. Neurosci. Rep.* 8, 198–210.
4. Coutinho, P., Barros, J., Zemmouri, R., Guimarães, J., Alves, C., Chorão, R., Lourenço, E., Ribeiro, P., Loureiro, J.L., Santos, J.V., et al. (1999). Clinical heterogeneity of autosomal recessive spastic paraplegias: analysis of 106 patients in 46 families. *Arch. Neurol.* 56, 943–949.
5. Erichsen, A.K., Koht, J., Stray-Pedersen, A., Abdelnoor, M., and Tallaksen, C.M. (2009). Prevalence of hereditary ataxia and spastic paraplegia in southeast Norway: a population-based study. *Brain* 132, 1577–1588.
6. Dion, P.A., Daoud, H., and Rouleau, G.A. (2009). Genetics of motor neuron disorders: new insights into pathogenic mechanisms. *Nat. Rev. Genet.* 10, 769–782.
7. Finsterer, J., Löscher, W., Quasthoff, S., Wanschitz, J., Auer-Grumbach, M., and Stevanin, G. (2012). Hereditary spastic paraplegias with autosomal dominant, recessive, X-linked, or maternal trait of inheritance. *J. Neurol. Sci.* 318, 1–18.
8. Fink, J.K. (2013). Hereditary spastic paraplegia: clinico-pathologic features and emerging molecular mechanisms. *Acta Neuropathol.* 126, 307–328.
9. Blackstone, C., O’Kane, C.J., and Reid, E. (2011). Hereditary spastic paraplegias: membrane traffic and the motor pathway. *Nat. Rev. Neurosci.* 12, 31–42.
10. Montenegro, G., Rebelo, A.P., Connell, J., Allison, R., Babalini, C., D’Aloia, M., Montieri, P., Schüle, R., Ishiura, H., Price, J., et al. (2012). Mutations in the ER-shaping protein reticulon 2 cause the axon-degenerative disorder hereditary spastic paraplegia type 12. *J. Clin. Invest.* 122, 538–544.
11. Züchner, S., Wang, G., Tran-Viet, K.N., Nance, M.A., Gaskell, P.C., Vance, J.M., Ashley-Koch, A.E., and Pericak-Vance, M.A. (2006). Mutations in the novel mitochondrial protein REEP1 cause hereditary spastic paraplegia type 31. *Am. J. Hum. Genet.* 79, 365–369.
12. Voeltz, G.K., Prinz, W.A., Shibata, Y., Rist, J.M., and Rapoport, T.A. (2006). A class of membrane proteins shaping the tubular endoplasmic reticulum. *Cell* 124, 573–586.
13. Shibata, Y., Shemesh, T., Prinz, W.A., Palazzo, A.F., Kozlov, M.M., and Rapoport, T.A. (2010). Mechanisms determining the morphology of the peripheral ER. *Cell* 143, 774–788.
14. Beetz, C., Koch, N., Khundadze, M., Zimmer, G., Nietzsche, S., Hertel, N., Huebner, A.K., Mumtaz, R., Schweizer, M., Dirren, E., et al. (2013). A spastic paraplegia mouse model reveals REEP1-dependent ER shaping. *J. Clin. Invest.* 123, 4273–4282.
15. Park, S.H., Zhu, P.P., Parker, R.L., and Blackstone, C. (2010). Hereditary spastic paraplegia proteins REEP1, spastin, and atlastin-1 coordinate microtubule interactions with the tubular ER network. *J. Clin. Invest.* 120, 1097–1110.
16. Schüle, R., Holland-Letz, T., Klimpe, S., Kassubek, J., Klopstock, T., Mall, V., Otto, S., Winner, B., and Schöls, L. (2006). The Spastic Paraplegia Rating Scale (SPRS): a reliable and valid measure of disease severity. *Neurology* 67, 430–434.
17. Tesson, C., Nawara, M., Salih, M.A., Rossignol, R., Zaki, M.S., Al Balwi, M., Schüle, R., Mignot, C., Obre, E., Bouhouche, A., et al. (2012). Alteration of fatty-acid-metabolizing enzymes affects mitochondrial form and function in hereditary spastic paraplegia. *Am. J. Hum. Genet.* 91, 1051–1064.
18. Schüle, R., Bonin, M., Dürr, A., Forlani, S., Sperfeld, A.D., Klimpe, S., Mueller, J.C., Seibel, A., van de Warrenburg, B.P., Bauer, P., and Schöls, L. (2009). Autosomal dominant spastic paraplegia with peripheral neuropathy maps to chr12q23-24. *Neurology* 72, 1893–1898.
19. Gonzalez, M.A., Lebrigio, R.F., Van Booven, D., Ulloa, R.H., Powell, E., Spezziani, F., Tekin, M., Schüle, R., and Züchner, S. (2013). GENomes Management Application (GEM.app): a new software tool for large-scale collaborative genome analysis. *Hum. Mutat.* 34, 842–846.
20. McKenna, A., Hanna, M., Banks, E., Sivachenko, A., Cibulskis, K., Kernysky, A., Garimella, K., Altshuler, D., Gabriel, S., Daly, M., and DePristo, M.A. (2010). The Genome Analysis Toolkit: a MapReduce framework for analyzing next-generation DNA sequencing data. *Genome Res.* 20, 1297–1303.
21. Meijer, I.A., Cossette, P., Roussel, J., Benard, M., Toupin, S., and Rouleau, G.A. (2004). A novel locus for pure recessive hereditary spastic paraplegia maps to 10q22.1-10q24.1. *Ann. Neurol.* 56, 579–582.
22. Dursun, U., Koroglu, C., Kocasoy Orhan, E., Ugur, S.A., and Tolun, A. (2009). Autosomal recessive spastic paraplegia (SPG45) with mental retardation maps to 10q24.3-q25.1. *Neurogenetics* 10, 325–331.
23. Steinmüller, R., Lantigua-Cruz, A., Garcia-Garcia, R., Kostrzewa, M., Steinberger, D., and Müller, U. (1997). Evidence of a third locus in X-linked recessive spastic paraplegia. *Hum. Genet.* 100, 287–289.
24. Kumar, K.R., Blair, N.F., Vandebona, H., Liang, C., Ng, K., Sharpe, D.M., Grünwald, A., Gölitz, U., Saviouk, V., Rolfs, A., et al. (2013). Targeted next generation sequencing in SPAST-negative hereditary spastic paraplegia. *J. Neurol.* 260, 2516–2522.
25. Goizet, C., Depienne, C., Benard, G., Boukhris, A., Mundwiler, E., Solé, G., Couprie, I., Pilliod, J., Martin-Négrier, M.L., Fedirko, E., et al. (2011). REEP1 mutations in SPG31: frequency, mutational spectrum, and potential association with mitochondrial morpho-functional dysfunction. *Hum. Mutat.* 32, 1118–1127.
26. Schlang, K.J., Arning, L., Epplen, J.T., and Stemmler, S. (2008). Autosomal dominant hereditary spastic paraplegia: novel mutations in the REEP1 gene (SPG31). *BMC Med. Genet.* 9, 71.
27. Beetz, C., Schüle, R., Deconinck, T., Tran-Viet, K.N., Zhu, H., Kremer, B.P., Frants, S.G., van Zelst-Stams, W.A., Byrne, P., Otto, S., et al. (2008). REEP1 mutation spectrum and genotype/phenotype correlation in hereditary spastic paraplegia type 31. *Brain* 131, 1078–1086.
28. Ilegems, E., Iwatsuki, K., Kokrashvili, Z., Benard, O., Nino-miya, Y., and Margolskee, R.F. (2010). REEP2 enhances sweet receptor function by recruitment to lipid rafts. *J. Neurosci.* 30, 13774–13783.
29. Shibata, Y., Voss, C., Rist, J.M., Hu, J., Rapoport, T.A., Prinz, W.A., and Voeltz, G.K. (2008). The reticulon and DP1/Yop1p proteins form immobile oligomers in the tubular endoplasmic reticulum. *J. Biol. Chem.* 283, 18892–18904.
30. Schlaitz, A.L., Thompson, J., Wong, C.C., Yates, J.R., 3rd, and Heald, R. (2013). REEP3/4 ensure endoplasmic reticulum clearance from metaphase chromatin and proper nuclear envelope architecture. *Dev. Cell* 26, 315–323.
31. Darios, F., Corti, O., Lücking, C.B., Hampe, C., Muriel, M.P., Abbas, N., Gu, W.J., Hirsch, E.C., Rooney, T., Ruberg, M., and Brice, A. (2003). Parkin prevents mitochondrial swelling

- and cytochrome c release in mitochondria-dependent cell death. *Hum. Mol. Genet.* 12, 517–526.
32. Darios, F., Wasser, C., Shakirzyanova, A., Giniatullin, A., Goodman, K., Munoz-Bravo, J.L., Raingo, J., Jorgacevski, J., Kreft, M., Zorec, R., et al. (2009). Sphingosine facilitates SNARE complex assembly and activates synaptic vesicle exocytosis. *Neuron* 62, 683–694.
33. Björk, S., Hurt, C.M., Ho, V.K., and Angelotti, T. (2013). REEPs are membrane shaping adapter proteins that modulate specific G protein-coupled receptor trafficking by affecting ER cargo capacity. *PLoS ONE* 8, e76366.
34. Lausch, E., Keppler, R., Hilbert, K., Cormier-Daire, V., Nikkel, S., Nishimura, G., Unger, S., Spranger, J., Superti-Furga, A., and Zabel, B. (2009). Mutations in MMP9 and MMP13 determine the mode of inheritance and the clinical spectrum of metaphyseal anadysplasia. *Am. J. Hum. Genet.* 85, 168–178.
35. Klebe, S., Depienne, C., Gerber, S., Challe, G., Anheim, M., Charles, P., Fedirko, E., Lejeune, E., Cottineau, J., Brusco, A., et al. (2012). Spastic paraplegia gene 7 in patients with spasticity and/or optic neuropathy. *Brain* 135, 2980–2993.